25th ABCM International Congress of Mechanical Engineering
October 20-25, 2019, Uberlândia, MG, Brazil

COB-2019-0540
THERMODYNAMIC OPTIMIZATION OF A HEAT EXCHANGER USED IN THERMAL CYCLES APPLICABLE FOR SPACE SYSTEMS

Elvis Falcão de Araújo
Guilherme Borges Ribeiro
Lamartine Nogueira Frutuoso Guimarães
Instituto de Estudos Avancados
Trevo Coronel Aviador José Alberto Albano do Amarante, 01 - Putim, São José dos Campos - SP, 12228-001
falcao@ieav.cta.br
gbribeiro@ieav.cta.br
guimarae@ieav.cta.br

Abstract. *Nuclear power conversion in space has been approached in several different ways since the first space missions, with the advent of concepts such as thermoelectric, thermionic and thermodynamic conversion. Nowadays, thermal cycles are under greater focus for being capable of providing higher conversion efficiencies. In this context, one of the main concerns of designers and engineers is the trade-off between power and mass. Therefore, this work aims the optimization of a recuperator used in a regenerative Closed Brayton Cycle applied for power conversion in the project of a fast nuclear microreactor under the Brazilian Air Force strategic program. It is a cross-flow, shell-and-tube heat exchanger with a matrix of tubes distributed in a staggered configuration. In this work, the number of tubes and the mass flow rate are varied. The number of tubes distributed axially is fixed in 4, while the quantity around the axis varies between 5, 7, 9, 12 and 16 tubes. The fluid and solid materials are respectively He-Xe (40 g/mol) and Alloy 617. The optimization studies are supported by CFD and entropy generation minimization. Optimum mass flow rates are obtained for all the geometries at the points of minimum entropy generation number, around which lie the ranges of tested mass flow rates. Geometry selection is performed using the ratio of minimum entropy generation number to effectiveness at the optimum mass flow rate associated to a given geometry as performance evaluation criteria and assessing its behavior with exchanger mass. This analysis leads to the optimum design point at the geometry of 9 tubes around recuperator axis, with 0.1 kg/s mass flow rate, 0.059 entropy generation number and 0.2312 effectiveness.*

Keywords: *Recuperator, CFD, entropy, heat transfer, pressure drop*

1. INTRODUCTION

Nuclear reactors are currently seen as the best power source for space exploration vehicles due to several design advantages in comparison to its alternatives (solar, chemical and radioisotope), such as compact size, low mass, long operating lifetime, resistance to hostile environments and high system reliability (MCclure and Poston, 2013), being the best solution for electricity generation in terrestrial orbits that require 40 kWe electrical power or higher (Borges and Sielawa, 1992). The power conversion of space nuclear powered system designs along the last years had been mostly performed by thermoelectric, thermionic and thermodynamic means. Nowadays, the majority of designs in this area have preferred the thermodynamic option due to its capacity of providing higher conversion efficiencies (Araújo and Guimarães, 2018).

Thermal cycles possess a wide range of applications in multiple engineering fields, being used for power conversion in plants using several thermal energy inputs (solar, thermoelectric, nuclear, etc) and for propulsion and power generation in vehicles developed in the naval, auto, aeronautical and space industries. Stirling, Rankine and Brayton cycles are strongly used in several nuclear designs, where Stirling engines are primarily used in low power ranges (< 40 kWe) (Briggs *et al.*, 2014; Toro and Lior, 2017). In high power level regimes, Rankine cycles are mainly applied for power conversion in terrestrial and naval nuclear reactors, while Brayton cycles are more suitable for space nuclear power systems since it can provide a higher power-to-radiator area ratio ψ (Tarlecki *et al.*, 2007; Toro and Lior, 2017), which is critical for mission success due to system overall size minimization.

The majority of current plants use regeneration for allowing higher cycle first law efficiencies (Gallo and El-Genk, 2009; Ahn and Lee, 2014; Goodarzi, 2016; Olumayegun *et al.*, 2017). In regenerative cycles, a certain quantity of heat abstracted from the turbine outlet fluid is utilized to heat the one in the compressor outlet, which pre-heats fluid in the hot heat exchanger inlet and diminishes the demand of thermal energy from the heat source for a given net power output

and consequently increases the efficiency of the thermodynamic cycle (Sonntag *et al.*, 1998). The regenerator is a heat exchanger that makes thermal contact between the turbine and compressor outlets. The role of this component in a thermodynamic cycle is displayed graphically in Fig. 1, which shows a schematic drawing and the temperature-entropy diagram of a regenerative Brayton cycle.

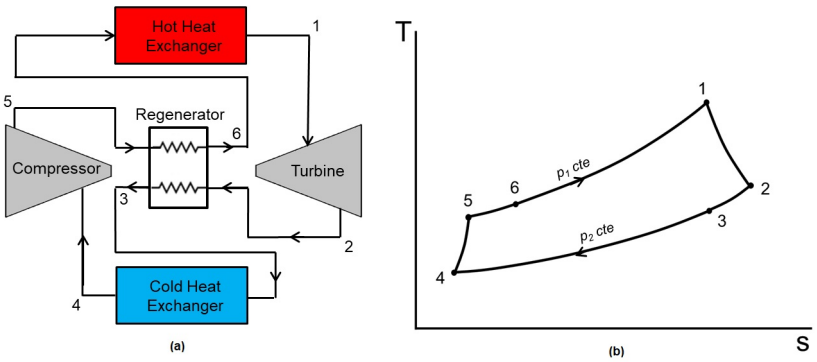

Figure 1: The ideal regenerative Brayton cycle schematic drawing (a) and temperature-entropy chart (b) (Sonntag *et al.*, 1998).

Improvements in regeneration performance have a great impact on power conversion efficiency, thus an optimization study in the regenerator can provide a considerable plant performance gain. The search for more compact heat exchangers has been occurring to fulfill industry needs for smaller and lighter equipment, mainly in areas such as biomedicine, fuel processing and aerospace (Dixit and Ghost, 2015). Regeneration is critical for space applications, where low mass and volume are desired for the plant so more science payload can be launched. In this context, a second-law based assessment technique, namely Entropy Generation Minimization (Bejan, 1982), has recently found applicability in several novel works of the thermal field. Furthermore, this method has recently been proven to be useful for analysis and optimization in a wide range of scientific areas.

The EGM method is an engineering tool used to design and optimize devices and installations based on principles of thermodynamics, heat transfer, fluids mechanics and other transport phenomena with the objective of minimizing the thermodynamic imperfection caused by heat transfer, mass transfer, fluid flow and other processes (Bejan, 2006). If $\dot{W}$ is the heat transfer rate of a given open system and T_0 is the environment temperature, the merger between the first and second laws of thermodynamics leads to a law of proportionality between the work destroyed through thermodynamic irreversibility $\dot{W}_{lost}$, also called Lost Available Work (LAW), and the entropy generation rate $\dot{S}_{gen}$, namely the Guoy-Stodola theorem, which is mathematically expressed by

$$\dot{W}_{lost} = \dot{W}_{rev} - \dot{W} = T_0 \dot{S}_{gen} \tag{1}$$

This theorem leads to the conclusion that system available work destruction can be measured by the amount of entropy generation. Furthermore, by invoking the reversible limit shown in the first equality, it is possible to determine the upper limit to the work transfer rate of which a given system can be capable (Jin, 2017). The EGM method is carried out subject to physical constraints that are responsible for the irreversible operation of the device. Thus, to minimize the entropy generation rate of a given system, one must find an expression for $\dot{S}_{gen}$ which attaches the thermodynamic nonideality to any system physical characteristic, which requires the use of relations between temperature differences and heat transfer rates, and between pressure gradients and mass flow rates. Therefore, the designer must rely on heat transfer and fluid mechanics principles, in addition to thermodynamics (Bejan, 2006).

In the context of the growing demand for performance assessment and improvement in compact dynamic thermal cycles and considering that the space nuclear technology state-of-the-art is converging to smaller plants with high power-to-mass ratios, this work proposes a new methodology for analysis and optimization of a Closed Brayton Cycle regenerator through CFD modelling and Second law analysis. The regenerator under study is a cross-flow, shell-and-tube heat exchanger. Like will be shown later, it possesses multiple tubes whose quantity is not fixed by design. Besides, as it is part of a closed cycle with no bleed, inlet mass flow rates $\dot{m}$ are necessarily the same for both streams. The optimization performed here is based on a parametrical study where both number of tubes and mass flow rate are varied. The exchanger geometry is brought to the commercial CFD software Ansys Fluent, where a physical model is built using data from the literature. The flow inside the recuperator is then solved with the Finite Volume Method (FVM) (Patankar, 1980). Several geometries are tested, and multiple simulations are performed with variable mass flow rate for each one of them, with further thermodynamic analysis in the post processing. The optimum geometry and mass flow rate are then searched based on entropy generation number and effectiveness.

2. METHODOLOGY

2.1 Numerical Model

The regenerator under study is a shell-and-tube heat exchanger with its tubes disposed around its center in a staggered distribution and a 30° deviation from the radial orientation. The cold domain fills the exchanger tube side, while the hot stream fills the shell side. The bodies within this model are solely the streams and the tubes through which heat is conducted. The number of tubes in the axis is fixed in 4 so the regenerator volume remains constant, while the number around the axis is variable. Figure 2(a) shows an isometric view of the used geometry for mesh independence check, which possesses 3 tubes distributed azimuthally. It includes arrows to indicate the flow path along the fluid domain in both streams. Figure 2(b) shows the main model dimensions and gives a clearer view of domain geometry. In the parametrical study, the number of tubes around the axis varies between 5, 7, 9, 12 and 16.

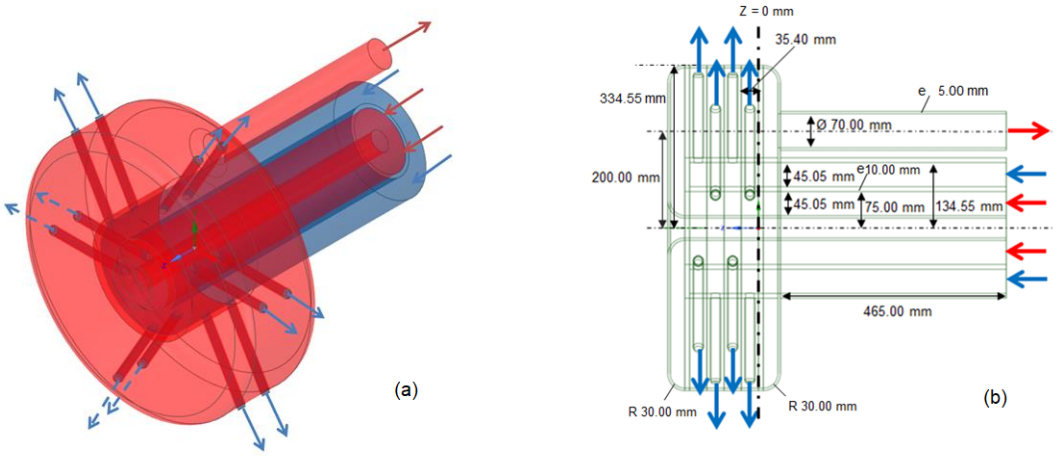

Figure 2: (a) Regenerator fluid domains, where the blue and red colors indicate respectively the cold and hot domains. (b) Regenerator geometry details, with blue and red arrows indicating the terminals of the cold and hot domains, respectively.

The CFD models use mass flow inlets and pressure outlets as boundary conditions. The physical model draws inspiration from a NASA nuclear electric propulsion (NEP) based space mission concept started in 2003 using a 200 kWe Brayton engine, namely the Prometheus project (Ashcroft and Eshelman, 2007). The inlet temperatures are 538 K and 943 K, while the solid and fluid materials are respectively alloy 617 and helium-xenon mixture with 40 g/mol molecular weight. Properties of the solid and fluid materials are displayed in Tab. 1. It can be seen that the properties vary with temperature. A linear dependence is assumed in this model as the literature provides property data only at the displayed temperatures. Atmospheric pressure (101325 Pa) is assumed on the outlets. Heat transfer is only considered through the tube walls, therefore any other system surface is considered adiabatic. The incompressible ideal gas model expressed by the state equation (Eq. (2)) defines fluid density ρ. This assumption is valid because flow Mach Number M is less than 0.3 for all simulations (subsonic flow) (ANSYS, 2016). The ideal gas assumption is valid for low molecular weight He-Xe (< 60 g/mol) in low pressures and high temperatures (El-Genk, 2009). This is a steady and turbulent flow with with 5 % turbulence intensity, which is lumped into the numerical treatment with the $k-\epsilon$ model. In addition to the state and turbulence equations, the flow is goverened by the balances of mass (Eq. (2)), momentum (Eq. (3)) and energy (Eq. (5)). The spatial discretization schemes are linear for pressure and first order upwind for velocity, energy, turbulent kinetic energy and dissipation rate.

$$\rho = \frac{p_{op}}{RT} \tag{2}$$

$$\frac{\partial \rho}{\partial t} + \nabla \cdot (\rho \vec{u}) = 0 \tag{3}$$

$$\rho \left[\frac{\partial \vec{u}}{\partial t} + (\vec{u} \cdot \nabla)\vec{u} \right] = -\nabla p + \nabla \cdot \bar{\tau} + \rho \vec{F} \tag{4}$$

$$\rho \left[\frac{\partial c_p T}{\partial t} + \nabla \cdot (c_p T \vec{u}) \right] = -\frac{Dp}{Dt} + \nabla \cdot (k \nabla T) + \phi \tag{5}$$

Where p_{op} responds for the operation pressure (which is 101325 Pa in this case), R is the ideal gas constant (J/kgK), variable t is time (s), the term u is particle velocity (m/s), variable p is pressure (Pa), the term $\bar{\tau}$ is the shear stress

tensor (Pa), variable $\overrightarrow{F}$ is the overall sum of body forces acting on the particle (N), the term c_p is the constant pressure specific heat (J/kgK), variable k is the heat conduction coefficient (W/mK) and ϕ represents energy lost through viscous dissipation, also known as dissipation function (Pa/s).

Table 1: Properties of the solid and fluid materials used in physical model.

Material	Alloy 617	He-Xe (400 K)	He-Xe (1200 K)
Thermal conductivity [W/mK]	18.825	0.08409	0.18340
Specific heat [J/kgK]	419	535.7	519.7
Density [kg/m^3]	8360	State Equation	State Equation
Viscosity [μPas]	-	32.857	74.286

2.2 Performance Parameters

This subsection is devoted to the description of the parameters used in this work to evaluate the regenerator performance: the entropy generation number and the effectiveness. The evaluation of these parameters uses terminal pressures and termperatures that are extracted from the solved CFD cases. This work assumes a balanced counterflow exchanger in the ideal limit of small pressure and temperature gradients with constant thermal properties throughout domain flow. In a heat exchanger, thermodynamical losses occur by entropy generation due to the flow pressure drop along its segments and the heat transfer between them. The total entropy generation is expressed by equation (6) (Bejan, 2006), where the first two terms in the right-hand side respond for the entropy generation due to heat transfer, while the last two terms refer to entropy generated by pressure drop.

$$\dot{S}_{gen} = (\dot{m}c_p)_c \ln \frac{T_{c,out}}{T_{h,in}} + (\dot{m}c_p)_h \ln \frac{T_{h,out}}{T_{h,in}} - (\dot{m}R)_c \ln \frac{P_{c,out}}{P_{c,in}} - (\dot{m}R)_h \ln \frac{P_{h,out}}{P_{h,in}} \tag{6}$$

The entropy generation number N_s is a non-dimensional parameter used to extrapolate irreversibility evaluations from one exchanger to others of the same type with different sizes. The pressure drop and heat transfer entropy generation numbers for heat exchangers are respectively expressed by equations (7) and (8). The total entropy generation number is the sum of its contributions due to pressure drop and heat transfer.

$$N_{s,\Delta p} = \frac{\dot{S}_{gen,\Delta p}}{\dot{m}c_p} \tag{7}$$

$$N_{s,q} = \frac{\dot{S}_{gen,q}}{\dot{m}c_p} \tag{8}$$

The effectiveness ε is a non-dimensional metric used to evaluate the regenerator thermal performance defined as a ratio of the actual heat transfer rate from the hot fluid to the cold fluid to the maximum possible heat transfer rate thermodynamically permitted, which would be achieved in an ideal exchanger of infinite heat transfer area. It is expressed by equation (9) for any flow arrangement, where $\dot{C}$ is the flow heat capacity rate. In the particular case of this work, where it is assumed that both streams have the same heat capacity rates, the effectiveness expression is reduced to equation (10).

$$\varepsilon = \frac{\dot{C}_h(T_{h,in} - T_{h,out})}{\dot{C}_{min}(T_{h,in} - T_{c,in})} = \frac{\dot{C}_c(T_{c,out} - T_{c,in})}{\dot{C}_{min}(T_{h,in} - T_{c,in})} \tag{9}$$

$$\varepsilon = \frac{T_{h,in} - T_{h,out}}{T_{h,in} - T_{c,in}} = \frac{T_{c,out} - T_{c,in}}{T_{h,in} - T_{c,in}} \tag{10}$$

3. RESULTS

3.1 Mesh Quality Test

The grids used for the simulations follow a pattern in which elements of the tubes and inlets are hexahedral, while tetrahedral elements are used in the other regions due to geometrical difficulties. Besides, three layers of prismatic elements are used on domain surfaces to increase boundary layer catch precision. A linear relationship is defined between element size in the interior of a tube l and in all other regions, such as the entire mesh is defined by element size inside a tube. In order to find a numerically efficient mesh which could provide an accurate solution without excessive refinement (increasing computational cost), the temperature curve of 26 evenly spaced points along the centerline of a tube is evaluated for various simulations with fixed geometry (3 tubes around the axis) and mass flow rate $\dot{m}$ (0.1 kg/s) and variable

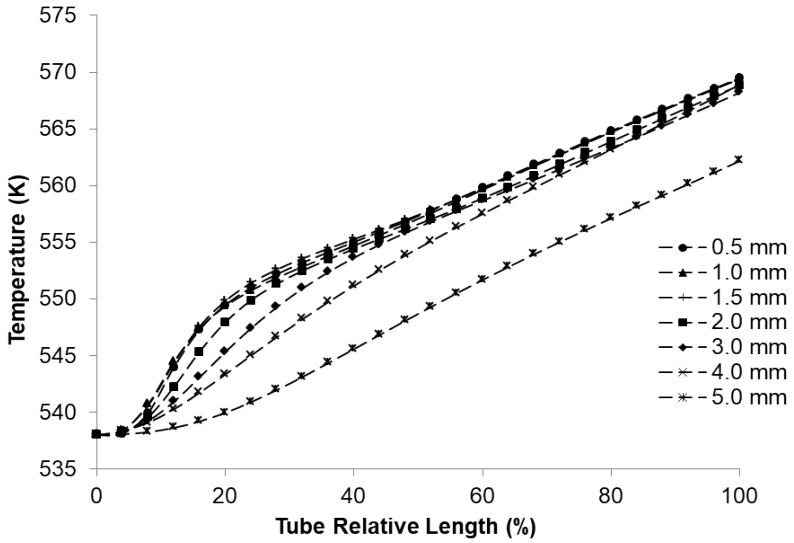

Figure 3: Temperature profiles obtained for multiple simulations with different tube interior mesh element size.

Table 2: Number of elements in function of tube interior element size.

l [mm]	Number of elements [-]
5	984510
4	1254307
3	1747957
2	3521590
1	15821218
0.5	36549790

tube interior element size, so that the independence of this parameter with mesh refinement can be assessed. The resulting plots are shown in fig. 3. Table 2 shows the number of elements for the used meshes in this study.

The figure-of-merit expressed by equation (11) is defined as the relative error between the mesh results of two consecutive grids in the refinement scale. Using this metric, the criterion for grid selection is the coarser mesh in a group of three consecutive meshes where the errors e_1 and e_2 are both less than 5 %. According to table 3 , the mesh with l = 1.5 mm is the best one for the parametrical study.

$$e = \max_{0 \leq i \leq 100} \frac{T_{g1}^{i} - T_{g2}^{i}}{T_{g2}^{100} - T_{g2}^{0}} \tag{11}$$

Table 3: Relative error in function of tube interior element size.

l [mm]	e [%]
5	21.83
4	8.94
3	8.50
2	7.17
1.5	2.36
1.0	2.41
0.5	-

3.2 Entropy Generation Number

As mentioned before, in a heat exchanger, the total entropy generation number results from the sum of its contributories from heat transfer in a finite temperature gradient and pressure drop. The $N_{s,\Delta p}$ rises with flow velocity due to the enlargement of reversible pressure drop due to flow contraction in both streams and also head losses through viscous dissipation, momentum rate change or flow separation due to exchanger geometrical features, while $N_{s,q}$ falls with flow velocity because particles are less exposed to the highest heat tranfer driving forces (temperature differences) in higher

velocity regimes, which reduces temperature gradients in both streams. The resultant total N_s is than expected to have a minimum value when plotted against flow velocity, Reynolds number, or mass flow rate. Figure 4 shows the total N_s results. The optimum design point for each geometry is also indicated. It can be seen that the optimum mass flow rates increase with exchanger number of tubes, as well as the N_s associated to it, which is a consequence of the heat transfer augmentation caused by increase in tubes quantity, which increases the heat transfer parcel of entropy generation.

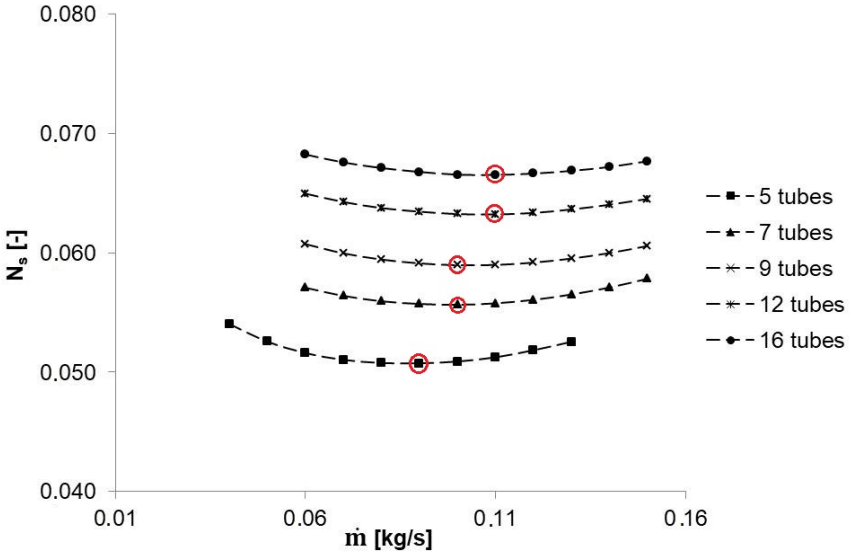

Figure 4: Influence of tubes quantity around the axis in total entropy generation number with the optimum design points circuled in red.

3.3 Effectiveness

The dependence between effectiveness and mass flow rates for multiple exchanger geometries is described by the curves of fig. 5. The effectiveness values decrease with mass flow rate and increase with number of tubes, showing a slight rise rate decrease as the number of tubes grows. Like discussed before, both effects are expected because flow velocity increase is responsible for the reduction of temperature variation in both streams, and increase in number of tubes augments heat transfer area, which causes the opposite effect.

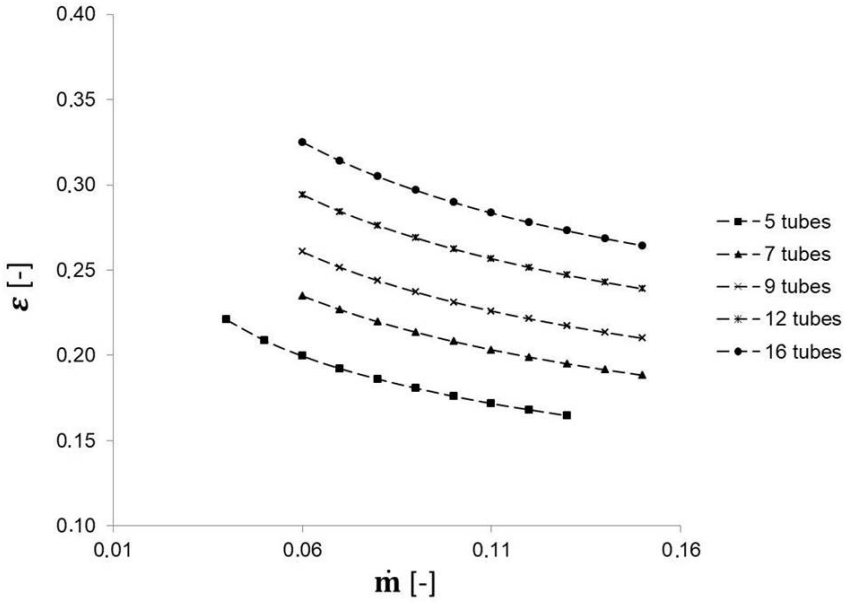

Figure 5: Influence of number of tubes around the axis in effectiveness.

3.4 Geometry Selection

The analysis of N_s and ε shows that both parameters increase with number of tubes in exchanger geometry, which reveals a contradictory performance behavior with this parameter when taking these metrics as criteria, because N_s responds for lost available work and must be minimized, while ε measures heat transfer performance and is desired to maximize. The figure-of-merit N_s/ε is used as auxiliary performance evaluation criterion for geometry selection. It can be deducted that this parameter is inversely proportional to exchanger performance. Like mentioned before, the device under study is desired to serve as the regenerator of a Closed Brayton Cycle applicable for a space reactor, so mass is a critical parameter which must also be optimized in order to diminish power demand for system launch. Figure shows the relation between N_s/ε and mass of exchanger structure, which is proportional to the number of tubes. These values are only taken in the optimum design points showed in fig. 4, which reveals the minimum N_s mass flow rates for a fixed geometry. This procedure is adopted because the relative variation of N_s with mass flow rate is considerably higher than that of ε when number of tubes is constant.

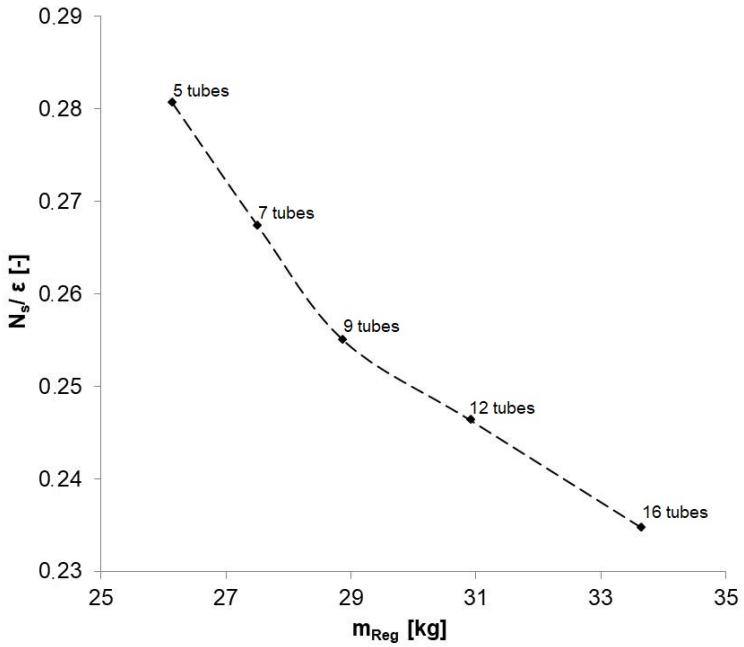

Figure 6: Ratio of entropy generation number and effectiveness variation with regenerator mass, with geometries indicated by the number of tubes around the axis.

It can be seen that there is a reduction in the rate of N_s/ε with regenerator mass when the number of tubes around the axis is higher than 9, which occurs because both N_s and ε increase with number of tubes in a decreasing rate. If more tubes were tested, both parameters would stabilize, thus the PEC would reach a minimum value. Therefore, the geometry with 9 tubes around regenerator is the most suitable for usage in the Closed Brayton Cycle for providing the best trade-off between performance and mass. The optimum design point is: $\dot{m}$ = 0.10 kg/s, N_{tubes} = 36, N_s = 0.059, $\dot{S}_{gen}$ = 3.12 W/K, $\dot{W}_{lost}$ = 929.76 W and ε = 0.2312.

4. CONCLUSIONS

The entropy generation minimization is used in this work to optimize a crossflow heat exchanger to be used as the regenerator of a regenerative Closed Brayton Cycle applicable for space reactors. First, the heat transfer and fluid flow in this device is simulated in a CFD platform over a physical model which draws inspiration from the NASA Prometheus project. The Second Law analysis is then performed by applying the balanced counterflow expressions given by Bejan (1982) using the terminal pressures and temperatures of the two streams as inputs and varying the exchanger mass flow rate and number of tubes in order to perform a parametrical study.

In addition to the thermodynamical study, the heat transfer performance is assessed through the exchanger effectiveness, which is obtained from the terminal temperatures extracted from the solved CFD cases. Mass flow rate is optimized for each geometry at the points of minimum N_s, while number of tubes is optimized through the analysis of the dependence between N_s/ε and regenerator mass.

It can be observed that the minimum N_s mass flow rates increase with number of tubes, as well as the entropy generation numbers associated to these design points, which is explained by the higher order of magnitude of the $N_{s,q}$

contribution to the total entropy generation number than that of the one from pressure drop. The rise of minimum N_s mass flow rate with number of tubes is an effect of the greater cold flow cross sectional area, which lowers pressure drop through flow contraction and rises the required mass flow rate for the flow to achive the optimum pressure drop. The effectiveness results decrease with mass flow rates and rise with number of tubes, which is expected from heat transfer theory because of the increase of heat capacity rate in the former case and of the heat transfer area in the latter. The used performance evaluation criteria for geometry selection lead to the geometry with 36 tubes for being the one with the best equilibrium between low N_s/ε and regenerator mass. In this geometry, the optimum N_s mass flow rate is 0.10 kg/s.

5. RESPONSIBILITY NOTICE

The authors are the only responsible for the printed material included in this paper.

6. REFERENCES

Ahn, Y. and Lee, J.I., 2014. "Study of various brayton cycle designs for small modular sodium-cooled fast reactor". *Nuclear Engineering and Design*, Vol. 276, pp. 128–141.

Araújo, E.F. and Guimarães, L.N.F., 2018. "American Space Nuclear Electric Systems". *Journal of Aerospace Technology and Management*, Vol. 10.

Ashcroft, J. and Eshelman, C., 2007. "Summary of NR Program Prometheus Efforts". In *Proceedings of the Space Technology and Applications International Forum*. Space Technology and Applications International Forum, American Institute of Physics, pp. 497–521.

Bejan, A., 1982. *Entropy Generation through heat and fluid flow*. John Wiley & Sons, Boulder, Colorado, USA, 2nd edition.

Bejan, A., 2006. *Advanced Engineering Thermodynamics*. John Wiley & Sons, Durham, North Carolina, USA, 3rd edition.

Borges, E.M. and Sielawa, J.T., 1992. "Simulação e controle de escoamento do circuito primário de refrigeração do reator espacial sp-100". In *IV Congresso Geral de Energia Nuclear*. Brazil.

Briggs, M.H., Gibson, M.A. and Geng, S.M., 2014. "Status update for the fission surface power technology demonstration unit". In *Nuclear and Emerging Technologies for Space*. USA.

Dixit, T. and Ghost, I., 2015. "Review of micro- and mini-channel heat sinks and heat exchangers for single phase fluids". *Renewable & Sustainable Energy*, Vol. 41, pp. 1298–1311.

El-Genk, M.S., 2009. "Deployment hystory and design considerations for space reactor power systems". *Acta Astronautica*, Vol. 64, pp. 833–849.

Gallo, B.M. and El-Genk, M.S., 2009. "Brayton Rotating Units for space reactor power systems". *Energy Conversion and Management*, Vol. 50, pp. 2210–2232.

Goodarzi, M., 2016. "Usefulness analysis on regenerator and heat exchanger in brayton & inverse brayton cycles at moderate pressure ratio operation". *Energy Conversion and Management*, Vol. 126, pp. 982–990.

Jin, Y., 2017. "Second Law Analysis: A Powerful Tool for Analyzing Computational Fluid Dynamics (CFD) Results". *Entropy*, Vol. 19, pp. 679–681.

MCclure, P.R. and Poston, D., 2013. "Design and testing of small nuclear reactors for defense applications". In *Invited Talk to ANS Trinity Section*. USA.

Olumayegun, O., Wang, M. and Kelsall, G., 2017. "Thermodynamic analysis and preliminary design of closed brayton cycle using nitrogenas working fluid and coupled to small modular sodium-cooled fast reactor (sm-sfr)". *Applied Energy*, Vol. 191, pp. 436–453.

Patankar, S.V., 1980. *Numerical Heat Transfer and Fluid Flow*. McGraw-Hill, New York, USA.

Sonntag, R.E., Borgnakke, C. and Wylen, G.J.V., 1998. *Fundamentals of Thermodynamics*. John Wiley & Sons, USA, 5th edition.

Tarlecki, J., Lior, N. and Zhang, N., 2007. "Analysis of thermal cycles and working fluids for power generation in space". *Energy Conversion & Management*, Vol. 48, pp. 2864–2878.

Toro, C. and Lior, N., 2017. "Analysis and comparison of solar-heat driven stirling, brayton and rankine cycles for space power generation". *Energy*, Vol. 120, pp. 549–564.